INSTITUTE OF PHYSICS PUBLISHING PLASMA PHYSICS AND CONTROLLED FUSION

Plasma Phys. Control. Fusion **47** (2005) 657–669 doi:10.1088/0741-3335/47/4/006

A gyrokinetic electron and fully kinetic ion plasma simulation model

Yu Lin[1,4], **Xueyi Wang**[1], **Zhihong Lin**[2] **and Liu Chen**[2,3]

[1] Physics Department, Auburn University, Auburn, AL, USA
[2] Department of Physics and Astronomy, University of California, Irvine, CA, USA
[3] Department of Physics, Zhejiang University, Hangzhou, People's Republic of China

E-mail: ylin@physics.auburn.edu

Received 1 October 2004, in final form 12 November 2004
Published 4 March 2005
Online at stacks.iop.org/PPCF/47/657

Abstract

A novel new kinetic simulation model has been developed to investigate dynamics in collisionless plasmas. In this model, the electrons are treated as gyrokinetic (GK) particles and ions are treated as fully kinetic (FK) particles. In the GK-electron and FK-ion (GKe/FKi) plasma simulation model, the rapid electron cyclotron motion is removed, while keeping finite electron Larmor radii, realistic electron-to-ion mass ratio, wave–particle interactions, and off-diagonal components of the electron pressure tensor. The model is particularly suitable for plasma dynamics with wave frequencies lower than the electron gyrofrequency, and for problems in which the wave modes ranging from Alfvén waves to lower-hybrid/whistler waves need to be handled on an equal footing. Using this model, the computation power can be significantly improved over that of the existing full-particle codes. The GKe/FKi model, furthermore, can also handle physics with realistic electron-to-ion mass ratio and dynamic processes on the global Alfvén time/spatial scales. With respect to the hybrid (i.e. FK ion and fluid electron) model, the GKe/FKi model has the advantage that important electron kinetic physics, such as wave–particle resonances and finite electron Larmor radius effects, are included. The simulation model has been successfully benchmarked for linear waves in uniform plasmas against analytic dispersion relation.

1. Introduction

Numerical simulation has proven to be a powerful tool in understanding the kinetic physics of various fundamental plasma processes, in which the plasma dynamics is usually of nonlinear

[4] Author to whom any correspondence should be addressed.

nature under realistic conditions. There has been, however, a dilemma between the available computing power and the requirement in the resolution of relevant physics.

On the one hand, the physics of many interesting kinetic processes requires resolving both ion and electron time scales, in order to understand the collisionless dissipation, i.e. wave–particle interaction, involved in an integrated global-scale system. For example, to understand the physics of collisionless fast magnetic reconnection [1,2], which is a fundamental process in fusion [3–5] and space [6] plasmas, one needs to resolve finite electron Larmor radius effects, consider electron wave–particle resonance (i.e. Landau damping), and include electron's off-diagonal pressure terms, whereas the spatial and temporal scales of the reconnection process range from the short electron scales to global Alfvén scales. Another example is compressional Alfvén waves or eigenmodes (CAEs) in toroidal fusion devices excited by energetic ions produced in heating experiments or by fusion alpha particles [7]. Here, we need to resolve the ion cyclotron time scale and also include electron Landau and transient time damping as main damping mechanisms, which provide the crucial instability threshold conditions.

On the other hand, it is rather difficult to include all the disparate temporal and spatial scales of both electrons and ions in the calculation of a global system due to the constraints of available computing power. Existing full-particle simulations [8–10] and hybrid-particle simulations [11,12] are examples of solving kinetic physics on either local scale or global scale, respectively. The purpose of this paper is to develop an innovative new plasma simulation model, which includes both ion and electron particle kinetics in an electromagnetic system of collisionless plasmas and is computationally efficient. In the following, we address the necessity for this new model in detail by discussing some existing kinetic models.

Full-particle simulations have been utilized for decades, e.g. to investigate the triggering mechanism of magnetic reconnection [8–10, 13–16], in which electrons generally determine the conditions for breakdown of the frozen-in field line condition of collisionless plasmas and thus the occurrence of reconnection. In the full-particle codes, both the electrons and the ions are treated as fully kinetic (FK) particles. Due to disparate temporal and spatial scales between electrons and ions, most of the full-particle simulations have to employ unrealistically high electron-to-ion mass ratio, m_e/m_i, in order to accommodate available computing resources. An artificially large mass ratio may significantly affect, due to electrostatic effects, the nonlinear growth of the reconnection. Also due to the limited computing resources, the domains of most full-particle simulations have been limited to a few or a few tens of the ion Larmor radii, and simulation time much less than the global Alfvén time scale. Moreover, the majority of the work on kinetic structure and wave activities in the reconnection region has been based on the case with a zero guide magnetic field, which is definitely not appropriate in fusion plasmas.

Another kinetic approach often used, e.g. again in studies of reconnection, is the hybrid simulation, in which the ions are treated as FK particles, but the electrons are treated as a massless resistive fluid. In general, the hybrid codes do not resolve the small spatial and time scales associated with the electron mass, and have often been used to simulate global-scale structures associated with the ion dynamics [11, 17]. Thus, the electron kinetic effects are absent in the hybrid model. Electron wave–particle interactions can be treated in a drift kinetic electron model [18], which ignores the electron finite gyroradius and polarization effects. Since we need to include the off-diagonal electron pressure terms which are associated with finite electron gyroradius effects, the drift kinetic electron model is thus also inadequate to our purpose.

Motivated by the above inadequacies in the existing kinetic simulation models, we have developed an innovative new simulation model, in which the electron dynamics is determined by the gyrokinetic (GK) equations [19–21] and the ions obey the FK Vlasov equation. In the GK-electron and FK-ion (GKe/FKi) simulation, the rapid electron cyclotron motion is removed

while finite Larmor radius effects are retained [22]. This treatment results in a larger time step and allows us to treat the realistic electron-to-ion mass ratio and finite electron Larmor radii. The computation power can thus be significantly improved as compared with that of the full-particle codes. In addition, the simulation model is also amenable to massively parallel computation [23] and thus offers the exciting prospect of solving the reconnection physics in a global-scale system for a long-time evolution. The new model can be implemented in a particle-in-cell code or Vlasov code, or in a perturbative (δf) simulation.

The new simulation model requires that the gyro-kinetic approximation is valid for electrons, and thus is particularly suitable for the dynamics with wave frequency $\omega < \Omega_e$ and $k_\parallel < k_\perp$, where Ω_e is the electron gyrofrequency, and $k_\parallel$ and $k_\perp$ are the wave numbers parallel and perpendicular to the magnetic field, respectively. Wave modes relevant to many applications [2, 24], e.g. magnetohydrodynamic (MHD) modes, the obliquely propagating whistler/lower-hybrid waves, modified two-stream instabilities, and kinetic Alfvén waves, fall inside this range of dynamic scales.

In this paper, the GKe/FKi electromagnetic simulation model is presented. Then, as a necessary first step in developing this model to its fullest nonlinear physics, the benchmark against linear physics is presented. Analytical linear dispersion relation based on the GKe/FKi model is derived, and the results are compared with that from the standard FK theory and that from a new particle simulation code using the GKe/FKi model. It is shown that the model can indeed recover precisely the physics of various wave modes of interest, including, among others, the fast magnetosonic/whistler/lower-hybrid waves and Alfvén waves.

The outline of this paper is as follows. Section 2 describes the formulation of the simulation model. The theoretical benchmark of the GKe/FKi model is presented in section 3, and the benchmark of the numerical code is shown in section 4. Finally, a summary and discussions are given in section 5.

2. Description of GKe/FKi simulation model

The new GKe/FKi simulation model is developed by treating ions fully kinetically and the electrons with GK approximations. For the FK ions, the dynamics is governed by the Vlasov equation in six-dimensional phase space $(\boldsymbol{x}, \boldsymbol{v})$

$$\frac{\partial f_i}{\partial t} + \boldsymbol{v} \cdot \frac{\partial f_i}{\partial \boldsymbol{x}} + \frac{q_i}{m_i}\left(\boldsymbol{E} + \frac{1}{c}\boldsymbol{v} \times \boldsymbol{B}\right) \cdot \frac{\partial f_i}{\partial \boldsymbol{v}} = 0. \tag{1}$$

Here, f_i is ion distribution function, m_i is the ion mass, q_i is the ion charge, $\boldsymbol{E}$ is the electric field, and $\boldsymbol{B}$ is the magnetic field. In the present model, we adopt the particle-in-cell scheme [25]. Thus, f_i is represented by a group of particles that adequately sample the phase space volume

$$f_i(\boldsymbol{x}, \boldsymbol{v}, t) = \sum_j \delta[\boldsymbol{x} - \boldsymbol{x}_j(t)]\delta[\boldsymbol{v} - \boldsymbol{v}_j(t)], \tag{2}$$

where the index j represents individual particles. Given initial conditions at time $t = 0$ for particles and fields, the evolution of f_i is determined by ion motion under self-consistent electromagnetic fields, i.e.

$$\frac{\mathrm{d}\boldsymbol{v}}{\mathrm{d}t} = \frac{q_i}{m_i}(\boldsymbol{E} + \boldsymbol{v} \times \boldsymbol{B}), \tag{3}$$

$$\frac{\mathrm{d}\boldsymbol{x}}{\mathrm{d}t} = \boldsymbol{v}. \tag{4}$$

The number density and current density, n_i and $\boldsymbol{J}_\mathrm{i}$, are obtained from the velocity moments of f_i, i.e.

$$n_\mathrm{i} = \int f_\mathrm{i}\,\mathrm{d}^3v = \sum_j \delta(\boldsymbol{x} - \boldsymbol{x}_j), \tag{5}$$

$$\boldsymbol{J}_\mathrm{i} = q_\mathrm{i}\int \boldsymbol{v} f_\mathrm{i}\,\mathrm{d}^3v = q_\mathrm{i}\sum_j \boldsymbol{v}_j\delta(\boldsymbol{x} - \boldsymbol{x}_j) \tag{6}$$

and are deposited to a mesh of spatial grids.

For electrons, the difficulty in this conventional particle simulation approach is that the parallel grid size is limited by plasma Debye length, and the time step is limited by frequency of electron plasma oscillation or electron cyclotron motion. We, however, intend to have simulation size much larger than ion skin depth and simulation time much longer than the Alfvén time. Therefore the small electron–ion mass ratio introduces extreme computational challenge. Since the modes of interest have frequencies much smaller than Ω_e, and yet the finite electron Larmor radius effects need to be retained for off-diagonal pressure terms, we treat the electrons using a GK approach. By assuming $k_\perp \gg k_\parallel$, which is generally true for many processes such as magnetic reconnection and Alfvén instabilities in tokamak plasma, we can further suppress the high frequency electron plasma oscillation. This is valid even for $\Omega_\mathrm{e}^2 \sim \omega_\mathrm{pe}^2$, a typical parameter regime of fusion plasmas, where ω_pe is the electron plasma frequency.

We formally adopt the following GK ordering for electrons

$$\frac{\omega}{\Omega_\mathrm{e}} \sim \frac{\rho_\mathrm{e}}{L} \sim k_\parallel\rho_\mathrm{e} \sim \frac{\delta B}{B} \sim \epsilon, \tag{7}$$

$$k_\perp\rho_\mathrm{e} \sim 1. \tag{8}$$

Here, $\rho_\mathrm{e} = v_\mathrm{te}/\Omega_\mathrm{e}$ is the electron Larmor radius, $v_\mathrm{te} = \sqrt{T_\mathrm{e}/m_\mathrm{e}}$ is the electron thermal speed, L is the macroscopic background plasma scale length, δB is the perturbed magnetic field on the microscopic wave scale lengths, and ϵ is a smallness parameter. We can now make a coordinate transformation from particle coordinates $(\boldsymbol{x}, \boldsymbol{v})$ to gyrocentre coordinates $(\boldsymbol{R}, p_\parallel, \mu, \zeta)$, where $\boldsymbol{R} = (\boldsymbol{x} - \rho)$ is the gyrocentre position with $\rho = (\boldsymbol{b}\times\boldsymbol{v}_{\perp\mathrm{e}})/\Omega_\mathrm{e}$ being the gyroradius vector, $p_\parallel = m_\mathrm{e}v_{\mathrm{e}\parallel} + q_\mathrm{e}A_\parallel/c$ the parallel canonical momentum of electrons, q_e the electron charge, $v_{\mathrm{e}\parallel}$ and $\boldsymbol{v}_{\mathrm{e}\perp}$ the parallel and perpendicular velocities of electrons, respectively, μ the magnetic moment, $\boldsymbol{b} = \boldsymbol{B}/B$, $\boldsymbol{B} = \bar{\boldsymbol{B}} + \delta\boldsymbol{B}$, $\bar{\boldsymbol{B}}$ the background magnetic field averaged over the spatial and temporal scales of wave perturbations, and $\delta\boldsymbol{B} = \nabla\times\boldsymbol{A}$ the perturbed magnetic field. The parallel direction is defined along the background magnetic field $\bar{\boldsymbol{B}}$. The following GK equation can be obtained by averaging the Vlasov equation over the gyrophase angle ζ

$$\frac{\partial F_\mathrm{e}}{\partial t} + \frac{\mathrm{d}\boldsymbol{R}}{\mathrm{d}t}\cdot\frac{\partial F_\mathrm{e}}{\partial \boldsymbol{R}} + \frac{\mathrm{d}p_\parallel}{\mathrm{d}t}\frac{\partial F_\mathrm{e}}{\partial p_\parallel} = 0, \tag{9}$$

where the upper-case variables are gyrocentre variables, and $F_\mathrm{e}(\boldsymbol{R}, p_\parallel, \mu)$ is the distribution function of electrons in the five-dimensional gyrocentre phase space. The gyrocentre equations of motion for $p_\parallel$ and $\boldsymbol{R}$ are [20, 21, 26]

$$\frac{\mathrm{d}p_\parallel}{\mathrm{d}t} = -\boldsymbol{b}^*\cdot[q_\mathrm{e}\langle\nabla\phi^*\rangle + \mu\nabla\bar{B}], \tag{10}$$

$$\frac{\mathrm{d}\boldsymbol{R}}{\mathrm{d}t} = v_{\mathrm{e}\parallel}\boldsymbol{b}^* + \frac{c}{q_\mathrm{e}\bar{B}}\bar{\boldsymbol{b}}\times[q_\mathrm{e}\langle\nabla\phi^*\rangle + \mu\nabla\bar{B}], \tag{11}$$

where $\boldsymbol{b}^* = \bar{\boldsymbol{b}} + (v_{e\parallel}/\Omega_e)\bar{\boldsymbol{b}} \times (\bar{\boldsymbol{b}} \cdot \nabla)\bar{\boldsymbol{b}}$, $\bar{\boldsymbol{b}} = \bar{\boldsymbol{B}}/\bar{B}$, $\phi^* = \phi - \boldsymbol{v} \cdot \boldsymbol{A}/c$, ϕ and A are perturbed scalar and vector potentials, respectively, and the operator $\langle \cdots \rangle$ represents gyro-averaging. The electron gyro-averaged guiding centre charge density and $p_\parallel$-current are

$$\langle N_e \rangle = \int F_e \, \mathrm{d}^3 v, \tag{12}$$

$$\langle J_{e\parallel} \rangle = \frac{q_e}{m_e} \int p_\parallel F_e \, \mathrm{d}^3 v. \tag{13}$$

In GK simulations, the gyro-averaging is carried out numerically on a discretized gyro-orbit in real space [27].

Before we proceed with the formulations, it should be pointed out that the GK equations (10) and (11), as in the standard nonlinear GK theory, are fully nonlinear, with the nonlinear terms valid to the first order of ω/Ω_e in the GK ordering. This 'first order' is only for $\delta B/B$ on the microscopic wave scale (e.g. ρ_e), such that nonlinear frequencies corresponding to the spatial scales of interest are, while much smaller than the electron gyrofrquency, comparable to the linear frequency.

In order to advance F_e and f_i, we need to calculate the perturbed potentials and fields from the Maxwell equations, which consists of the Poisson's equation and the Ampere's law, with the Coulomb gauge $\nabla \cdot \boldsymbol{A} = 0$. First, let us calculate the potentials. Following the nonlinear GK formalism [19, 22], and assuming for now the background electron distribution function $\bar{f}_e$ being isotropic, the Poisson's equation then becomes

$$\nabla_\perp^2 \phi = -4\pi (q_i n_i + q_e n_e), \tag{14}$$

where n_e is the electron number density, and, for $w = v^2/2$,

$$n_e = \frac{q_e}{m_e} \int \mathrm{d}^3 v \left(\frac{\partial \bar{f}_e}{\partial w} \right) \left[\phi - \langle \phi \rangle + \frac{1}{c} \langle \boldsymbol{v}_\perp \cdot \boldsymbol{A} \rangle \right] + \langle N_e \rangle. \tag{15}$$

Detailed derivations of equation (15), and the following equations (16) and (17), are given in the appendix. Note that $\bar{f}_e$ is assumed to be isotropic here in order to simplify the presentation of the main idea. GK theory, of course, allows an anisotropic distribution, and extensions to anisotropic plasmas are conceptually straightforward. Assuming $|\nabla_\perp^2| \gg |\nabla_\parallel^2|$, we have replaced $\nabla^2 \phi$ by $\nabla_\perp^2 \phi$ in equation (14) to suppress the undesirable high-frequency Langmuir oscillation along $\boldsymbol{B}$. For now, let us further simplify the simulation scheme by taking $|\rho_e \nabla_\perp| < 1$. Equation (14) along with equation (15) then become the following generalized GK Poisson's equation

$$\left(1 + \frac{\bar{\omega}_{pe}^2}{\bar{\Omega}_e^2} \right) \nabla_\perp^2 \phi + 4\pi \bar{n}_e q_e \frac{\delta B_\parallel}{\bar{B}} = -4\pi (q_i n_i + q_e \langle N_e \rangle), \tag{16}$$

where $\bar{n}_e$ is the spatially averaged electron density, $\delta B_\parallel = \bar{\boldsymbol{b}} \cdot \delta \boldsymbol{B}$, and the second and third terms on the left-hand side correspond to the electron density due to its perpendicular guiding-centre polarization drift of the electrostatic electric field and $\boldsymbol{E} \times \boldsymbol{B}$ drift associated with inductive electric field $\partial \boldsymbol{A}_\perp / \partial t$, respectively.

Since $\omega \ll \Omega_e$, we can calculate $\delta B_\parallel$ using electron force balance instead of the usual perpendicular Ampere's law, i.e. from

$$\nabla \cdot (n_e q_e \boldsymbol{E}) = \nabla \cdot \left[\nabla \cdot \boldsymbol{P}_e - \frac{1}{c} \boldsymbol{J}_e \times \boldsymbol{B} \right], \tag{17}$$

where

$$\boldsymbol{P}_{\mathrm{e}} = \left(\bar{n}_{\mathrm{e}} q_{\mathrm{e}} \rho_{\mathrm{e}}^2 \nabla_\perp^2 \phi + 2\bar{n}_{\mathrm{e}} T_{\mathrm{e}} \frac{\delta \overline{B}_\parallel}{\bar{B}}\right)\left(\boldsymbol{I} - \frac{1}{2}\bar{\boldsymbol{b}}\bar{\boldsymbol{b}}\right) + \langle \boldsymbol{P}_g \rangle, \tag{18}$$

$$\langle \boldsymbol{P}_g \rangle = \int m_{\mathrm{e}} \boldsymbol{v}\boldsymbol{v} F_{\mathrm{e}} \, \mathrm{d}^3 v, \tag{19}$$

and, analogous to the derivation of n_{e}, the first two terms in the expression for $\boldsymbol{P}_{\mathrm{e}}$ are due to the electron perpendicular guiding-centre drifts. Assume, for now, a zero background electric field, i.e. $\boldsymbol{E} = \delta\boldsymbol{E}$. Noting that $\delta\boldsymbol{E} = -\nabla\phi - (1/c)\partial\boldsymbol{A}/\partial t$, $\nabla \cdot \boldsymbol{A} = 0$, the electron current density $\boldsymbol{J}_{\mathrm{e}} = (c/4\pi)\nabla \times \boldsymbol{B} - \boldsymbol{J}_{\mathrm{i}}$ with $\boldsymbol{J}_{\mathrm{i}}$ being the ion current density, $|\nabla_\perp| \gg |\nabla_\parallel|$, and ignoring corresponding higher-order terms, equation (17) can then be shown, after some algebra, to yield

$$\nabla^2 \Psi = -\nabla \cdot \left(\nabla \cdot \boldsymbol{P}_{\mathrm{g}} + \frac{1}{c}\boldsymbol{J}_{\mathrm{i}} \times \boldsymbol{B}\right), \tag{20}$$

where, noting $\bar{n}_{\mathrm{e}} q_{\mathrm{e}} = -\bar{n}_{\mathrm{i}} q_{\mathrm{i}}$,

$$\Psi = \frac{(1 + \bar{\beta}_{\mathrm{e}})\bar{B}\delta B_\parallel}{4\pi} - \bar{n}_{\mathrm{i}} q_{\mathrm{i}} (1 + \rho_{\mathrm{e}}^2 \nabla_\perp^2)\phi. \tag{21}$$

Expressing $\delta B_\parallel$ in terms of Ψ, given by equation (21), the GK Poisson's equation, equation (16), can finally be expressed as

$$\left[\left(1 + \bar{\beta}_{\mathrm{e}} + \frac{\bar{\omega}_{\mathrm{pe}}^2}{\bar{\Omega}_{\mathrm{e}}^2}\right)\nabla_\perp^2 - \frac{\bar{\omega}_{\mathrm{pi}}^2}{\bar{V}_A^2}\right]\phi = -4\pi\left[(1 + \bar{\beta}_{\mathrm{e}})(q_{\mathrm{i}} n_{\mathrm{i}} + q_{\mathrm{e}}\langle N_{\mathrm{e}}\rangle) - \frac{4\pi\bar{n}_{\mathrm{i}} q_{\mathrm{i}}}{\bar{B}^2}\Psi\right], \tag{22}$$

where $\bar{\omega}_{\mathrm{pi}}$ and $\bar{V}_{\mathrm{A}}$ are the background ion plasma frequency and the Alfvén speed, respectively. Equations (20) and (22) completely determine Ψ, ϕ, and, thereby, $\delta B_\parallel$ via equation (21).

The perturbed potential $A_\parallel$, meanwhile, is given by the following parallel Ampere's law

$$\left(\nabla^2 - \frac{\omega_{\mathrm{pe}}^2}{c^2}\right) A_\parallel = -\frac{4\pi}{c}(J_{\mathrm{i}\parallel} + \langle J_{e\parallel}\rangle). \tag{23}$$

When the perpendicular wavelength is longer than the electron collisionless skin depth, equation (23) is difficult to solve, since the second terms on both sides dominate and nearly cancel each other. We find that this difficulty can be overcome by evaluating the time-dependent electron plasma frequency in the second term of the left-hand side, i.e. $\omega_{\mathrm{pe}}^2 = 4\pi\langle N_{\mathrm{e}}\rangle q_{\mathrm{e}}^2/m_{\mathrm{e}}$. In equation (23), the high-frequency electromagnetic radiation (light wave) is suppressed ($|\omega|^2 \ll |ck|^2$).

Given $A_\parallel$ and $\delta B_\parallel$, we can now proceed to calculate $\boldsymbol{A}$. Let us decompose $\boldsymbol{A}$ into three locally orthogonal components, i.e. $\boldsymbol{A} = \boldsymbol{A}_\perp + A_\parallel\bar{\boldsymbol{b}} + \nabla_\perp\xi$. $\boldsymbol{A}_\perp$ is then determined by the perpendicular Ampere's law

$$\nabla^2 \boldsymbol{A}_\perp = -\frac{4\pi}{c}\boldsymbol{J}_\perp, \tag{24}$$

with $\boldsymbol{J}_\perp = (c/4\pi)\nabla \times (\delta\boldsymbol{B}_\parallel)$. $\nabla_\perp\xi$, meanwhile, can be determined by the Coulomb gauge $\nabla \cdot \boldsymbol{A} = 0$ or $\nabla_\perp^2\xi = -\nabla \cdot (A_\parallel\bar{\boldsymbol{b}})$.

We now proceed to calculate the perturbed fields. With $\boldsymbol{A}$ being completely specified, the perturbed magnetic field $\delta\boldsymbol{B}$ is simply $\delta\boldsymbol{B} = \nabla \times \boldsymbol{A}$. Meanwhile, as in the usual hybrid simulation scheme [28], since $\omega \ll \Omega_{\mathrm{e}}$, the electric field $\boldsymbol{E}$ that goes into the ion equation of

motion can be calculated from the following electron force balance equation,

$$n_e q_e \delta \boldsymbol{E} = -\nabla \cdot \boldsymbol{P}_e - \frac{1}{c} \boldsymbol{J}_e \times \boldsymbol{B}. \tag{25}$$

The calculated $\delta \boldsymbol{E}$ and $\boldsymbol{B} = \bar{\boldsymbol{B}} + \delta \boldsymbol{B}$ can then be used to advance ions.

We note that an innovative as well as nontrivial feature of this simulation model is that the electron GK dynamics is advanced by ϕ and $\boldsymbol{A}$, while the ion FK dynamics is advanced by $\delta \boldsymbol{E}$ and $\boldsymbol{B}$. Again, as will be demonstrated by the following theoretical as well as numerical benchmarks, the accuracy of the present model is limited to wave dynamics with $|\omega/\Omega_e|$ and $|k_\parallel/k| < 1$. The largest possible time step in this model is, thus, limited by the mode frequency of interest or electron parallel Courant condition for numerical stability. The perpendicular grid size is on the order of electron gyroradius, and the parallel grid size is on the order of parallel wavelength, which is much larger than the Debye length in usual parameter regimes. Collisions can be added if necessary using a Monte Carlo method.

3. Theoretical benchmark

To verify that the present model contains relevant wave physics, we have, based on the linearized GKe/FKi equations, derived the corresponding analytical linear dispersion relation. The linear dispersion relation can be expressed as

$$\begin{vmatrix} \bar{\rho}_\phi - k_\perp^2 & \bar{\rho}_\psi - k_\perp^2 & \bar{\rho}_b \\ -\bar{J}_{\parallel\phi} & k^2 - \bar{J}_{\parallel\psi} & -\bar{J}_{\parallel b} \\ -\bar{J}_{y\phi} & -\bar{J}_{y\psi} & k^2 - \bar{J}_{yb} \end{vmatrix} = 0, \tag{26}$$

where $\bar{\rho}_\phi = \bar{\rho}_{\phi i} + \bar{\rho}_{\phi e}$, $\bar{\rho}_\psi = \bar{\rho}_{\psi i} + \bar{\rho}_{\psi e}$, $\bar{\rho}_b = \bar{\rho}_{bi} + \bar{\rho}_{be}$, $\bar{J}_{\parallel\phi} = \bar{J}_{\parallel\phi i} + \bar{J}_{\parallel\phi e}$, $\bar{J}_{\parallel\psi} = \bar{J}_{\parallel\psi i} + \bar{J}_{\parallel\psi e}$, $\bar{J}_{\parallel b} = \bar{J}_{\parallel bi} + \bar{J}_{\parallel be}$, $\bar{J}_{y\phi} = \bar{J}_{y\phi i} + \bar{J}_{y\phi e}$, $\bar{J}_{y\psi} = \bar{J}_{y\psi i} + \bar{J}_{y\psi e}$ and $\bar{J}_{yb} = \bar{J}_{ybi} + \bar{J}_{ybe}$.

Here, the ion terms, with the subscript 'i', are obtained in a way similar to that in the standard FK model [29]. The expressions, however, are different here because the field variables in the set of governing GKe/FKi equations are $(\phi, A_\parallel, \delta B_\parallel)$ and, correspondingly, Poisson's equation and Ampere's law have been employed. The ion terms are thus given by

$$\bar{\rho}_{\phi i} = -\frac{1}{\lambda_{Di}^2} \left[1 + \omega \sum_{n=-\infty}^{+\infty} A_{ni} \Gamma_{0n,i} \right], \tag{27}$$

where λ_{Di} is the ion Debye length, $A_{ni} = (1/\sqrt{2} k_\parallel v_{ti}) Z(\xi_{ni})$, v_{ti} is the ion thermal speed, $Z(\xi)$ is the plasma dispersion function, $\xi_{ni} = (\omega - n\Omega_i)/\sqrt{2} k_\parallel v_{ti}$, $\Gamma_{0n,i} = e^{-\lambda_i} I_n(\lambda_i)$, I_n is the modified Bessel function, and $\lambda_i = (k_\perp \rho_i)^2$;

$$\bar{\rho}_{\psi i} = -\frac{1}{\lambda_{Di}^2} \frac{k^2}{k_\perp^2} \left[\sum_{n=-\infty}^{+\infty} n\Omega_i A_{ni} \Gamma_{0n,i} \right], \tag{28}$$

$$\bar{\rho}_{bi} = -\frac{1}{\lambda_{Di}^2} \sum_{n=-\infty}^{+\infty} \omega A_{ni} \Gamma_{1n,i}, \tag{29}$$

where $\Gamma_{1n,i} = e^{-\lambda_i}(I_n - I_n')$,

$$\bar{J}_{\parallel\phi i} = -\frac{1}{\lambda_{Di}^2} \frac{\omega^2}{k_\parallel^2 c^2} \sum_{n=-\infty}^{+\infty} B_{ni} \Gamma_{0n,i}, \tag{30}$$

where $B_{ni} = 1 + \xi_{ni} Z(\xi_{ni})$,

$$\bar{J}_{\parallel\psi\mathrm{i}} = -\frac{1}{\lambda_{\mathrm{Di}}^2} \frac{\omega\Omega_{\mathrm{i}}}{k_\parallel^2 c^2} \frac{k^2}{k_\perp^2} \sum_{n=-\infty}^{+\infty} n B_{ni} \Gamma_{0n,\mathrm{i}}, \tag{31}$$

$$\bar{J}_{\parallel\mathrm{bi}} = -\frac{1}{\lambda_{\mathrm{Di}}^2} \frac{\omega^2}{k_\parallel^2 c^2} \sum_{n=-\infty}^{+\infty} B_{ni} \Gamma_{1n,\mathrm{i}}, \tag{32}$$

$$\bar{J}_{y\phi\mathrm{i}} = k_\perp^2 \frac{\beta_{\mathrm{i}}}{2} \sum_{n=-\infty}^{+\infty} \omega A_{ni} \Gamma_{1n,\mathrm{i}}, \tag{33}$$

$$\bar{J}_{y\psi\mathrm{i}} = k^2 \frac{\beta_{\mathrm{i}}}{2} \Omega_{\mathrm{i}} \sum_{n=-\infty}^{+\infty} n A_{ni} \Gamma_{1n,\mathrm{i}} \tag{34}$$

and

$$\bar{J}_{\mathrm{ybi}} = \frac{\omega_{\mathrm{pi}}^2}{c^2} \sum_{n=-\infty}^{+\infty} \omega A_{ni} \Gamma_{2n,\mathrm{i}}, \tag{35}$$

where $\Gamma_{2n,\mathrm{i}} = \mathrm{e}^{-\lambda_{\mathrm{i}}}[(n^2/\lambda_{\mathrm{i}}) I_n + 2\lambda_{\mathrm{i}}(I_n - I_n')]$.

The corresponding electron terms, on the other hand, are derived via the linearized GK equations [30, 31]. They can be written as

$$\bar{\rho}_{\phi\mathrm{e}} = -\frac{1}{\lambda_{\mathrm{De}}^2}[1 + \Gamma_{0,\mathrm{e}} \xi_{\mathrm{e}} Z_{\mathrm{e}}], \tag{36}$$

where $\xi_{\mathrm{e}} = (\omega/\sqrt{2} k_\parallel v_{\mathrm{te}})$, $Z_{\mathrm{e}} = Z(\xi_{\mathrm{e}})$, $\Gamma_{0,\mathrm{e}} = \mathrm{e}^{-\lambda_{\mathrm{e}}} I_0(\lambda_{\mathrm{e}})$ and $\lambda_{\mathrm{e}} = (k_\perp \rho_{\mathrm{e}})^2$, with v_{te} being the electron thermal speed,

$$\bar{\rho}_{\psi\mathrm{e}} = -\frac{1}{\lambda_{\mathrm{De}}^2} \frac{k^2}{k_\perp^2}[1 - \Gamma_{0,\mathrm{e}}], \tag{37}$$

where λ_{De} is the electron Debye length,

$$\bar{\rho}_{\mathrm{be}} = \frac{1}{\lambda_{\mathrm{De}}^2} \frac{T_{\mathrm{e}}}{T_{\mathrm{i}}} \Gamma_{1,\mathrm{e}} \xi_{\mathrm{e}} Z_{\mathrm{e}}, \tag{38}$$

where T_{e} and T_{i} are the electron and ion temperatures, respectively, and $\Gamma_{1,\mathrm{e}} = \mathrm{e}^{-\lambda_{\mathrm{e}}}[I_0 - I_0']$,

$$\bar{J}_{\parallel\phi\mathrm{e}} = -\frac{1}{\lambda_{\mathrm{De}}^2} \frac{\omega^2}{k_\parallel^2 c^2} \Gamma_{0,\mathrm{e}}(1 + \xi_{\mathrm{e}} Z_{\mathrm{e}}), \tag{39}$$

$$\bar{J}_{\parallel\psi\mathrm{e}} = 0, \tag{40}$$

$$\bar{J}_{\parallel\mathrm{be}} = \frac{1}{\lambda_{\mathrm{De}}^2} \frac{\omega^2}{k_\parallel^2 c^2} \frac{T_{\mathrm{e}}}{T_{\mathrm{i}}} \Gamma_{1,\mathrm{e}}(1 + \xi_{\mathrm{e}} Z_{\mathrm{e}}), \tag{41}$$

$$\bar{J}_{y\phi\mathrm{e}} = -k_\perp^2 \frac{\beta_{\mathrm{i}}}{2} \Gamma_{1,\mathrm{e}} \xi_{\mathrm{e}} Z_{\mathrm{e}}, \tag{42}$$

where β_{i} is the ion plasma beta,

$$\bar{J}_{y\psi\mathrm{e}} = k_\perp^2 \frac{\beta_{\mathrm{i}}}{2} \Gamma_{1,\mathrm{e}} \tag{43}$$

and

$$\bar{J}_{\mathrm{ybe}} = \frac{\omega_{\mathrm{pe}}^2}{c^2} \xi_{\mathrm{e}} Z_{\mathrm{e}} \Gamma_{2,\mathrm{e}}, \tag{44}$$

where $\Gamma_{2,\mathrm{e}} = \mathrm{e}^{-\lambda_{\mathrm{e}}}(2\lambda_{\mathrm{e}})(I_0 - I_0') = 2\lambda_{\mathrm{e}} \Gamma_{1,\mathrm{e}}$.

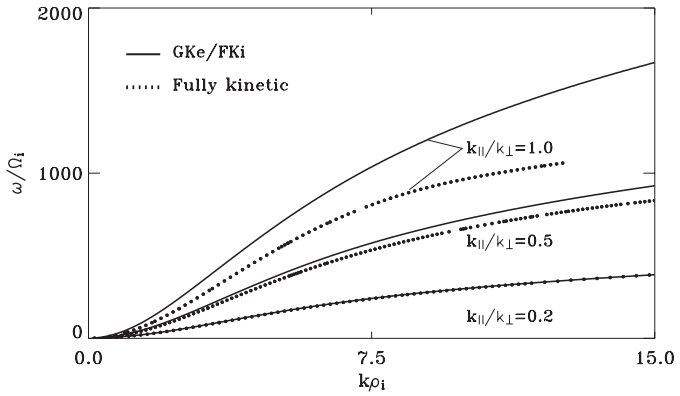

Figure 1. Analytical solutions of the linear dispersion relations for fast magnetosonic/whistler/lower-hybrid branch obtained from the GKe/FKi model (——) and the FK model (· · · · · ·, based on Stix [29]), for $\beta_e = \beta_i = 0.04$ and $k_\parallel/k_\perp = 0.2$, 0.5 and 1.0.

The solutions of the above dispersion relation are found to demonstrate the existence of wave modes of interests, such as kinetic Alfvén mode, lower-hybrid mode, and whistler mode, in addition to the three MHD modes. For $\omega \ll \Omega_e$, the solutions of these modes are exactly the same as those from the fully kinetic (i.e. FK electron and FK ion) model [29].

The solid lines in figure 1 show the analytical solution of the linear dispersion relation for fast magnetosonic/whistler/lower-hybrid mode branch obtained from our GKe/FKi model, for $\beta_e = \beta_i = 0.04$ and $\omega_{pe}/\Omega_e = 23$. The cases with $k_\parallel/k_\perp = 0.2$, 0.5 and 1.0 are plotted. For comparison, the corresponding solutions obtained from the FK model [29] are also shown with dotted lines. It is found that the GKe/FKi model is in excellent agreement with the FK model for $k_\parallel/k_\perp \leqslant 0.2$, and agrees reasonably well (with 10% error in ω at large $k\rho_e \sim 1$) to the FK model for $k_\parallel/k_\perp = 0.5$. As ω is getting close to Ω_e, the difference becomes more appreciable. The wave polarizations obtained from the GKe/FKi model also agree with those from the FK model. This analysis shows indeed that our new kinetic model is very accurate for dynamics with $\omega < \Omega_e$ and $k_\parallel < k_\perp$.

On the other hand, if the finite electron gyroradius is neglected in the analytical formulation shown above, i.e. treating electrons as drift kinetic particles, the corresponding analytical dispersion relation is found to produce dispersion curves significantly different from those of GK electrons. For the case with $k_\parallel/k_\perp \leqslant 0.2$, the drift kinetic electron/FK ion model produces a dispersion curve that deviates by ∼100% from the FK model at $k\rho_i \sim 10$.

4. Numerical benchmark

Various numerical approaches have been explored to implement the simulation model described in section 2. As a test, the particle-in-cell code has been run till approximately $60\Omega_i^{-1}$ for a one-dimensional uniform plasma. In the following, we present the benchmark of the code for a uniform plasma.

In the one-dimensional test runs, the grid size is chosen as $\sim 0.5-5\rho_e$, with a system length of about 60 ion Larmor radii. The mass ratio is $m_i/m_e = 1836$. A total of 100 electrons and 100 ions per grid are used. Initially, the particles are loaded uniformly on the grids, with a Maxwellian velocity distribution. The linear fluctuations at time $t > 0$ are due to the random noise, as in usual particle simulations. Total energy is well conserved, with a change of 0.01% at the end of the run. In the one-dimensional system, the wave vector $\boldsymbol{k}$ is along the x direction.

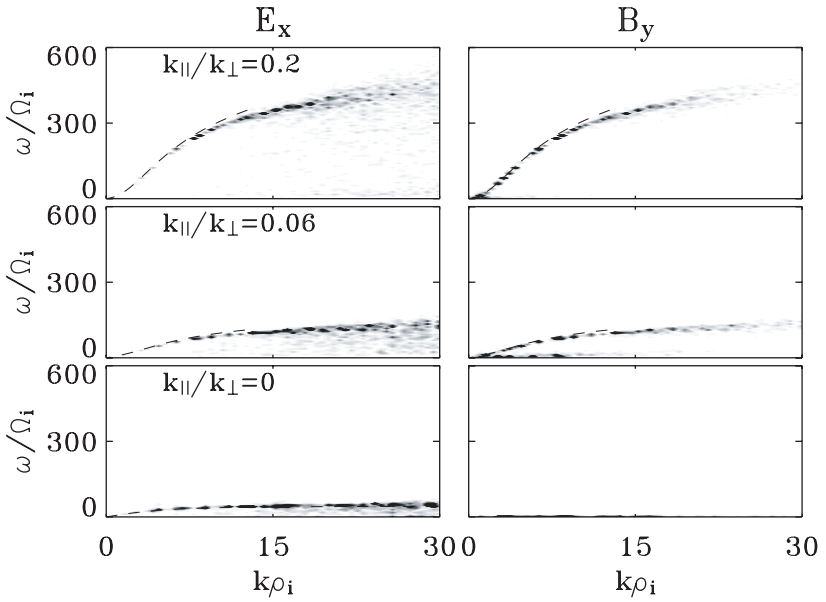

Figure 2. Linear dispersion relations obtained from the GKe/FKi simulation for the fast magnetosonic/whistler/lower-hybrid branch in a uniform system, for $k_\parallel/k_\perp = 0.2$ (top row), 0.06 (middle) and 0 (bottom). For comparison, the dashed lines show the corresponding dispersion relation derived analytically.

The background magnetic field $\boldsymbol{B}_0$ is in the xz plane and assumed to point to various directions relative to $\boldsymbol{k}$. The parallel canonical momentum of GK electrons and the velocities of ions are advanced in time by the second-order Runge–Kutta scheme, and so are the particle positions. The generalized GK Poisson's equation and the Ampere's laws are solved using fast fourier transform (FFT) or other finite-difference methods. The calculation is accurate to second-order in both time and space.

The code is benchmarked by comparisons between simulations of linear wave modes and the corresponding analytical solutions. Figure 2 shows the linear dispersion relations for the fast magnetosonic/whistler branch obtained from the simulation, again with $\beta_\mathrm{e} = \beta_\mathrm{i} = 0.04$. Plotted in figure 2 are the power spectra of E_x and B_y. The top, middle, and bottom rows present the cases with $k_\parallel/k_\perp = 0.2$, 0.06 and 0. The ratio of the peak power of the whistler mode to the power of the random noise is about 10^5. The dashed line in each case indicates the dispersion relation obtained from the theoretical analysis based on our GKe/FKi model, as described in section 3. In the simulation, the maximum wave amplitude in E_x is about 0.1 relative to $B_0 V_{\mathrm{A}0}$, and that in B_y is about 0.02 relative to B_0. It is seen that the numerical results agree very well with the theoretical analysis. The properties of wave polarization are also found to be consistent with the theoretical model. Note that at $k_\perp > \omega_{\mathrm{LH}}/V_\mathrm{A}$, where $\omega_{\mathrm{LH}} = \sqrt{\Omega_\mathrm{e}\Omega_\mathrm{i}}$ is the lower-hybrid frequency, the electromagnetic mode approaches the quasi-electrostatic lower-hybrid waves. In the case with $k_\parallel = 0$, there exist no magnetic fluctuations in δB_y.

In comparison, hybrid code can only handle the physics up to $k\rho_\mathrm{i} \sim 1$. For example, if the hybrid code with a massless electron ($m_\mathrm{e}/m_\mathrm{i} \simeq 0$) is forced to run a simulation with grid size $\ll\rho_\mathrm{i}$ (and time step $\ll\Omega_\mathrm{i}^{-1}$), the dispersion curve of the fast magnetosonic/whister branch significantly deviates from the theoretical curve at $k\rho_\mathrm{i} > 1.5$ and $\omega > 40\Omega_\mathrm{i}$ for the case with $k_\parallel/k_\perp = 0.2$, similar to the drift kinetic electron model. In this case, the dispersion curve of the hybrid model deviates from those of the FK mode and GKe/FKi mode by 200% at $k\rho_\mathrm{i} \sim 10$.

The code has also been examined for low frequency (i.e. $\omega < \Omega_i$) linear waves. The numerical results of the shear Alfvén (at $k\rho_i \ll 1$) and kinetic Alfvén (at $k\rho_i \sim 1$) modes, with perturbations mainly in $A_\parallel$, δB_y and ϕ, also agree very well with the analytical solution based on the GKe/FKi model, and the solution based on the FK model. The consistency between the theory and the numerical scheme has been confirmed for cases with values of β_e and β_i ranging from $O(10^{-2})$ to $O(1)$.

5. Summary and discussions

In summary, a new GKe/FKi plasma simulation model has been developed by seeking improvement in terms of both physics and computation power, with respect to the existing FK particle and hybrid codes. The new model, in which the electrons are treated as GK particles and ions are treated as FK particles, is particularly applicable to problems in which the wave modes ranging from magnetosonic and Alfvén waves to lower-hybrid/whistler waves need to be handled on an equal footing. To utilize this code, the simulated physical processes should be dominated by wave frequencies $\omega < \Omega_e$, and wave numbers $k_\parallel < k_\perp$. With fast electron gyromotion and Langmuir oscillations removed from the dynamics, the GKe/FKi model can readily employ realistic m_e/m_i mass ratio.

This novel simulation model, which allows a wide range of wave dynamics, should have broad applications in the topical areas of plasma macroscopic stability, microscopic turbulence, particle acceleration and heating by Alfvén or fast compressional waves, and in the application of massively parallel computing. More specifically, in addition to magnetic reconnection, another potential application of this simulation model is for the excitation and associated nonlinear physics of CAEs by energetic ions (e.g. beam ions and/or fusion alpha particles) in tokamak plasmas [7, 32]. Since CAE frequencies are typically in the ion cyclotron frequency range and could potentially heat thermal ions via stochastic processes [33, 34], full ion kinetics needs to be kept. On the other hand, electron Landau and/or transit-time damping are stabilizing and could provide the important instability threshold conditions. It is, therefore, crucial for the simulation model to also retain electron–wave kinetic interactions. The current GKe/FKi simulation scheme, again, should be suitable for this task.

The simulation model has been benchmarked theoretically and numerically for linear physics. So far, the benchmark shows that indeed the model can accurately resolve the physics of waves of interest. Benchmarking with respect to nonlinear physics remains to be carried out. In addition, to completely validate the code for nonlinear dynamics, more theoretical and numerical problems may need to be resolved. For example, the background fields also need to be determined in space and time if they are nonuniform and/or evolve with time. When the magnetic field direction is nonuniform, the inversion of the gradient operators need to be carried out locally using finite-difference or finite-element methods. While we leave these issues for future investigations, our initial success suggests that the present simulation model is rather promising and can well be applied to the investigation of a broad range of collisionless plasma dynamics.

Acknowledgments

This work was supported by NASA grant NAG5-12899 and NSF grant ATM-0213931 to Y Lin at Auburn University, NSF grant ATM-0335279 and DoE grant DE-FG-94ER54736 to L Chen, and DoE grant DE-FG02-03ER54694 to Z Lin. Y Lin was supported in part by an NSFC grant from China. L Chen was supported in part by Guangbiao Foundation of Zhejiang University.

The authors thank T S Hahm for insightful discussions. Computer resources were provided by the NERSC supercomputer centre and the Arctic Region Supercomputer centre.

Appendix A. Derivation of equations (15)–(17)

Employing the nonlinear gyrokinetic formalism of [19], the electron distribution function can be written, with subscript for species suppressed, as

$$f = \bar{f} + \frac{q\phi}{m}\frac{\partial \bar{f}}{\partial w} + T_{\rm g}^{-1}(\delta G), \tag{A1}$$

where $\bar{f}$ is the background distribution function taken to be isotropic for now, $w = v^2/2$, and $T_{\rm g}^{-1} = \exp(\rho \cdot \nabla_\perp)$ with ρ being the gyroradius vector corresponds to the inverse transformation from the gyrocentre to guiding-centre phase space. δG, meanwhile, obeys the following nonlinear GK equation

$$\left.\frac{\mathrm{d}}{\mathrm{d}t}\right|_{\rm g} \delta G = -\left[\frac{q}{m}\frac{\partial \bar{f}}{\partial w}\frac{\partial}{\partial t}\langle\phi^*\rangle + \dot{\boldsymbol{R}}\cdot\nabla\bar{f}\right], \tag{A2}$$

where $\mathrm{d}/\mathrm{d}t|_{\rm g} = \partial/\partial t + \dot{\boldsymbol{R}}\cdot\nabla$, with $\dot{\boldsymbol{R}}$ being given by equation (11), $\phi^* = T_{\rm g}(\phi - \boldsymbol{v}\cdot\boldsymbol{A}/c)$, and $\langle\cdots\rangle$ represents gyro-averaging. Removing the $\partial/\partial t$ term involving $\boldsymbol{A}_\perp$ and ϕ on the right-hand side of equation (A2) by letting

$$F(\mu, w, \boldsymbol{R}, t) = \delta G + \bar{f} + \frac{q}{m}\frac{\partial \bar{f}}{\partial w}\left\langle T_{\rm g}\left(\phi - \frac{1}{c}\boldsymbol{v}\cdot\boldsymbol{A}_\perp\right)\right\rangle, \tag{A3}$$

equation (A2) then becomes

$$\left.\frac{\mathrm{d}}{\mathrm{d}t}\right|_{\rm g} F - \frac{q}{m}\frac{\partial F}{\partial w}\left[\dot{\boldsymbol{R}}\cdot\nabla\left\langle T_{\rm g}\left(\phi - \frac{1}{c}\boldsymbol{v}\cdot\boldsymbol{A}_\perp\right)\right\rangle + \frac{v_\parallel}{c}\frac{\partial}{\partial t}\left\langle T_{\rm g}A_\parallel\right\rangle\right] = 0, \tag{A4}$$

where we have noted $\partial\bar{f}/\partial w \simeq \partial F/\partial w$. Changing the phase space variable from w to $p_\parallel = mv_\parallel + qA_\parallel/c$, F can then be shown, after some algebra, to satisfy equation (9), i.e.

$$\frac{\partial F}{\partial t} + \dot{\boldsymbol{R}}\cdot\frac{\partial F}{\partial \boldsymbol{R}} + \dot{p}_\parallel\frac{\partial F}{\partial p_\parallel} = 0. \tag{A5}$$

Noting equation (A3), equation (A1) can be expressed as

$$f = \frac{q}{m}\frac{\partial \bar{f}}{\partial w}\left[\phi - T_{\rm g}^{-1}\left\langle T_{\rm g}\left(\phi - \frac{1}{c}\boldsymbol{v}\cdot\boldsymbol{A}_\perp\right)\right\rangle\right] + T_{\rm g}^{-1}F. \tag{A6}$$

We also note that the same result has been derived by Brizard [26] for a Maxwellian background distribution function. Equation (15) readily follows equation (A6). Assuming $|\rho\cdot\nabla_\perp| < 1$, equation (A6) can be further approximated as

$$f \simeq -\frac{q}{m}\frac{\partial \bar{f}}{\partial w}\left[\left(\rho\cdot\nabla_\perp + \frac{1}{2}\rho\rho : \nabla_\perp\nabla_\perp + \frac{1}{4}\rho^2\nabla_\perp^2\right)\phi + \frac{mv_\perp^2}{2q}\frac{\delta B_\parallel}{\bar{B}}\right] + T_{\rm g}^{-1}F. \tag{A7}$$

From equation (A7), we can readily derive $n_{\rm e}$ and $\boldsymbol{P}_{\rm e}$ in, respectively, equations (16) and (17).

References

[1] Dungey J W 1961 *Phys. Rev. Lett.* **6** 47
[2] Petschek H E 1964 *AAS-NASA Symp. on the Physics of Solar Flares, NASA Spec. Publ. SP-50* (Washington, DC: National Aeronautics and Space Administration) pp 425–39
[3] Yamada M, Levintin F M, Pomphrey N, Budny R, Manickam J and Nagayama Y 1994 *Phys. Plasmas* **1** 3269
[4] Kadomtsev B B 1975 *J. Plasma Phys.* **1** 389

[5] Semenov I *et al* 2003 *Phys. Plasmas* **10** 664
[6] Hones E W Jr 1979 *Space Sci. Rev.* **23** 393
[7] Fredrickson E *et al* 2001 *Phys. Rev. Lett.* **87** 145001
[8] Hoshino M 1987 *J. Geophys. Res.* **92** 7368
[9] Shay M A and Drake J F 1998 *Geophys. Res. Lett.* **25** 3759
[10] Pritchett P L 2001 *J. Geophys. Res.* **106** 3783
[11] Lin Y and Swift D W 1996 *J. Geophys. Res.* **101** 19,859
[12] Belova E V, Davidson R C, Ji H and Yamada M 2004 *Phys. Plasmas* **11** 2523
[13] Terasawa T 1981 *J. Geophys. Res.* **86** 9007
[14] Mandt M E, Denton E R and Drake J F 1994 *Geophys. Res. Lett.* **21** 73
[15] Cai H J and Lee L C 1997 *Phys. Plasmas* **4** 590
[16] Hesse M and Winske D 1998 *J. Geophys. Res.* **103** 26479
[17] Nakamura M and Scholer M 2000 *J. Geophys. Res.* **105** 23179
[18] Tanaka M 1995 *Comput. Phys. Commun.* **87** 117
[19] Frieman E A and Chen L 1982 *Phys. Fluids* **25** 502
[20] Hahm T S, Lee W W and Brizard A 1988 *Phys. Fluids* **31** 1940
[21] Brizard A 1989 *J. Plasma Phys.* **41** 541
[22] Lee W W 1983 *Phys. Fluids* **26** 556
[23] Lin Z, Hahm T S, Lee W W, Tang W M and White R B 1998 *Science* **281** 1835
[24] Ji H, Terry S, Yamada M, Kulsrud R, Kuritsyn A and Ren Y 2004 *Phys. Rev. Lett.* **92** 115001
[25] Birdsall C K and Langdon A B 1991 *Plasma Physics via Computer Simulation* (Bristol: Institute of Physics)
[26] Brizard A 1992 *Phys. Fluids* B **4** 1213
[27] Lee W W 1987 *J. Comput. Phys.* **72** 243
[28] Swift D W 1996 *J. Comput. Phys.* **126** 109
[29] Stix T H 1992 *Waves in Plasmas* (New York: American Institute of Physics)
[30] Antonsen T M and Lane B 1980 *Phys. Fluids* **23** 1205
[31] Chen L and Hasegawa A 1991 *J. Geophys. Res.* **96** 1503
[32] Gorelenkov N N, Cheng C Z, Fredrickson E, Belova E, Gates D, Kaye S, Kramer G J, Nazikian R and White R B 2002 *Nucl. Fusion* **42** 977
[33] Chen L, Lin Z and White R B 2001 *Phys. Plasmas* **8** 4713
[34] Gates D, Gorelenkov N N and White R B 2001 *Phys. Rev. Lett.* **87** 205003